Propagation of Stress Waves in Fiber-Reinforced Composite Rods

T. R. TAUCHERT*
University of Kentucky, Lexington, Ken.

AND

F. C. MOON†
Princeton University, Princeton, N. J.

The mechanical behavior of fiber-reinforced composite materials subject to dynamic loadings is investigated. The elastic moduli and damping coefficients of glass-epoxy and boron-epoxy beams were determined from the frequencies and bandwidths of their resonances during lateral forced vibrations. Longitudinal stress pulses were generated in the composites by impact of lead pellets fired from a pneumatic rifle. Measured values of the velocity and attenuation of the pulses agree favorably with those based upon the vibration data and the assumption of linear viscoelastic behavior. Results of an exploratory study on the propagation of high-frequency waves in composites using an ultrasonic technique are also reported.

I. Introduction

A VAST quantity of literature on the subject of fiber-reinforced composite materials has accumulated in recent years. The great majority of the experimental investigations have been concerned with the static mechanical properties of the composites. Meanwhile little attention has been given to studying their dynamic behavior. A few noteworthy exceptions include: the recent investigations by Schultz and Tsai[1,2] on the dynamic moduli and damping properties of glass-epoxy beams; Abbott and Broutman's[3] measurements of the velocity of stress waves; Lifshitz'[4] vibration and wave propagation tests based upon experimental methods developed by Kolsky and coworkers[5,6]; and finally Assay et al.[7,8] ultrasonic wave velocity measurements on reinforced laminates.

The purpose of the research described in this paper has been to study the dynamic response of glass-epoxy and boron-epoxy composites. The effective complex moduli of these materials are obtained in Sec. II and used in Sec. III to predict the behavior of longitudinal stress pulses in thin rods. A comparison with measured pulse-propagation data is made. Preliminary results on the propagation of ultrasonic waves in the composite materials are given in Sec. IV, and concluding remarks are made in Sec. V.

II. Vibration Tests

A series of vibration tests were conducted in order to determine the dependence of the materials' complex moduli upon frequency. Thin cantilever-beam specimens were vibrated using a sinusoidal oscillator and an electromagnetic transducer (Fig. 1). Since the composites being investigated are nonmagnetic materials, a small ferromagnetic disc was glued to each sample in front of the transducer. The force oscillations were monitored by means of a capacitive transducer, the output of which was displayed on an oscilloscope. A thin strip of aluminum foil, glued to the face of the test specimen, served as the ground plate of the air-capacitor. The mass of this foil plus the mass of the ferro-magnetic disk represent a negligible addition to the specimen's total mass. A Brüel and Kjaer jig (Complex Modulus Apparatus, model 3930) was used to clamp the beam and to position the two transducers. When testing at the higher frequencies (5000–10,000 cps), where the small response required considerable amplification, a band-pass filter was used to reduce noise.

The specimens used in the vibration tests included both glass-fiber and boron-fiber unidirectionally reinforced epoxy composites. Glass-epoxy beams were machined from sheets of Minnesota Mining and Manufacturing Company "Scotchply" type 1002; the filaments in this material have a diameter of 0.038 mil, and represent approximately 64% (by weight) of the composite. Boron-epoxy specimens were cut from "Scotchply" type SP-272 panels. The diameter of the boron fibers is 4.0 mils, and the nominal fiber content is 68%. Typical dimensions of the beams were 8 in. long, 0.5 in. wide, and 0.05 in. thick.

The storage modulus E_1 (the real part of the composite's complex moduli $E^* = E_1 + iE_2$) was computed from the measured natural frequencies f_n using the relation‡

$$E_1 = 4\pi^2\mu l^4 f_n^2 / I(\beta_n l)^4 \qquad (1)$$

where μ is the mass per unit length, l the length and I the moment of inertia of the beam; β_n are the eigenvalues of the frequency equation governing the flexural vibrations. Shear deformation and rotary inertia effects were significant at the higher frequencies and were accounted for using the Timoshenko beam theory.

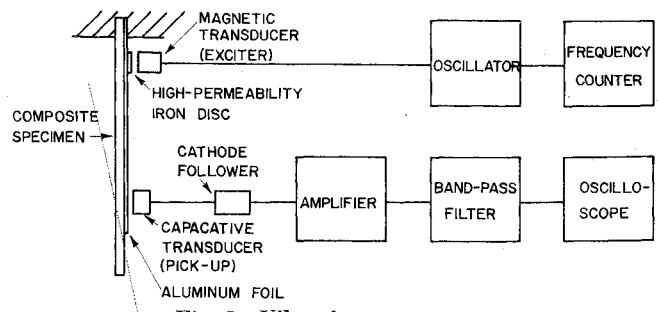

Fig. 1 Vibration apparatus.

Presented at AIAA/ASME 11th Structures, Structural Dynamics, and Materials Conference, Denver Colo., April 22–24, 1970 (no paper number; published in bound volume); submitted June 17, 1970; revision received November 9, 1970. The authors wish to thank the Hamilton Standard Division of United Aircraft Corporation for providing specially prepared boron-epoxy rod specimens. Supported by the U.S. Army Research Office-Durham.

* Associate Professor, Department of Engineering Mechanics.

† Assistant Professor, Department of Aerospace and Mechanical Sciences.

‡ Equation (1) is based upon the elastic beam theory. It is, however, applicable to viscoelastic materials which have relatively small damping; that is, materials for which $\tan\delta \ll 1$. Both composite materials studied herein fall into this class.

Table 1 Vibration data for a steel specimen

Mode	Frequency f_n, cps	f_n/f_1	Theoretical f_n/f_1	Modulus $E_1 \times 10^{-6}$, psi Classical	Timoshenko	Loss factor $\tan\delta \times 10^2$ Decay	Bandwidth
1	71.3	1.0	1.0	28.0	28.0	0.32	—
2	446	6.25	6.27	27.9	27.9	0.36	0.35
3	1250	17.5	17.5	28.1	28.1	0.28	0.29
4	2440	34.3	34.4	27.9	28.0	0.13	0.14
5	4030	56.7	56.8	27.8	28.0	0.17	0.18
6	5990	84.0	84.9	27.5	28.0	0.24	0.25
7	8360	117	119	27.5	27.8	—	0.25
8	11,100	156	158	27.4	27.9	—	—
9	14,200	199	203	27.2	27.9	—	—
10	10,700	249	253	27.0	27.9	—	—

Damping in the composite specimens was determined by observing the bandwidth Δf of the resonance curve; Δf denotes the width of the curve at 0.707 of its maximum amplitude. The damping is expressed in terms of the loss factor $\tan\delta$, where δ represents the angle by which the strain lags the stress during sinusoidal oscillations. This damping measure is related to the observed bandwidth by the relation

$$\tan\delta = \Delta f/f_n \qquad (2)$$

In order to ascertain the useful range of the experimental technique, the response of a steel specimen to forced vibrations was examined. The resulting data is presented in Table 1, wherein it is seen that resonant frequencies as high as 17,7000 cps (10th mode) can be measured. It was difficult, however, to get a clear output signal above 10,000 cps, and consequently the damping was not measured at frequencies greater than this value.

The ratio of each natural frequency f_n to the fundamental frequency f_1 is also given in the Table. Relatively good agreement exists between these experimental values and the theoretical values based upon classical beam theory. However, the moduli E_1 [computed from the measured frequencies using Eq. (1)] decrease slightly with increasing frequency. This decrease is due to the fact that Eq. (1) neglects the effects of shear deformation and rotary inertia. When these effects are taken into account by using the Timoshenko beam theory,[9] the value of E_1 is seen to be essentially independent of frequency, as expected. Henceforth, all reported values of E_1 will include this correction.

Values of the loss factor $\tan\delta$, computed from the measured bandwidths of the resonance curves using Eq. (2), are shown in the last column of the Table. For the purpose of comparison, the damping was also determined by observing the decay of free oscillations. This was accomplished by exciting the beam at a natural frequency, then switching off the driving current and recording the decay. The two methods are seen to give results which differ by less than 10% in all cases.

Vibration data for a glass-epoxy specimen is shown in Table 2. The data correspond to average values obtained in several independent tests on the same specimen. Measured values of the natural frequencies differed by less than 1% in each of the tests, and damping by less than about 10%. Tests on other glass-epoxy specimens gave similar results, although the loss factor sometimes differed by as much as 20% from one specimen to another. The data are in good agreement with the more extensive results for glass-epoxy composites presented by Schultz and Tsai.[1] These investigators observed a strong dependence of damping upon excitation amplitudes in the lowest few modes of vibration but not in the higher modes. In the present experiments the maximum strain amplitude did not exceed approximately 100μin./in., and within this range the damping appeared to be independent of the amplitude of vibration. As reported in Ref. 1, the damping in glass-epoxy tends to increase with frequency whereas the modulus is relatively constant.

Table 2 Vibration data for a glass-epoxy specimen

Mode	Frequency f_n, cps	f_n/f_1	Modulus $E_1 \times 10^{-6}$, psi	Loss factor $\tan\delta \times 10^2$
1	49.5	1.0	5.17	—
2	312	6.30	5.23	0.25
3	877	17.7	5.27	0.54
4	1712	34.6	5.28	0.51
5	2815	56.9	5.24	0.51
6	4176	84.4	5.13	0.70
7	5774	117	5.13	0.76
8	7596	153	5.06	1.00
9	9620	194	5.07	1.60

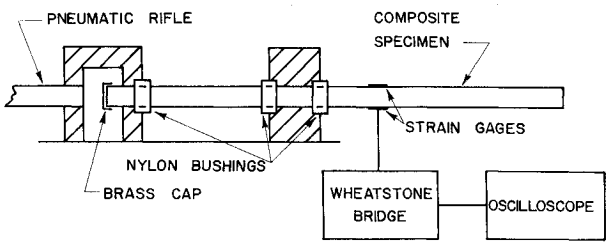

Fig. 2 Pulse-propagation apparatus.

Vibration tests on the boron-epoxy specimens yielded similar results. The moduli and loss factors for three different specimens are shown in Table 3. The first two beams were unidirectionally reinforced, with fibers in the longitudinal (0°) and transverse (90°) directions, respectively; the third beam was a cross-ply laminate (alternate 0° and 90° plies). Damping is slightly smaller in the first beam than in the longitudinal glass-epoxy specimen (Table 2). The loss factor for the beam with transverse fibers is approximately 5 to 8 times greater than that for the beam with longitudinal fibers; the cross-ply specimen has nearly the same damping as the longitudinal one.

The above data for the glass-epoxy and boron-epoxy specimens will be used in the following Section to predict the velocity and attenuation of longitudinal stress pulses in these composites.

III. Pulse Propagation Tests

The experimental apparatus which was used to generate pulses in the composite materials is similar to that suggested by Pao and Kowal.[10] A lead pellet, fired from a 20 calibre pneumatic rifle, impacted one end of a cylindrical specimen (Fig. 2). A small brass cap was affixed to the rod's impact end to prevent permanent damage to the specimen. Rigid body motion was restrained by nylon bushings, as shown in the figure. Strain was monitored using etched-foil-type gages; the signal from the initial pulse was used to trigger the oscilloscope which recorded the transient wave-forms.

Glass-epoxy specimens for the pulse propagation tests were machined from unidirectional sheets of Scotchply 1002, the same material as that used in the vibration tests. Boron-

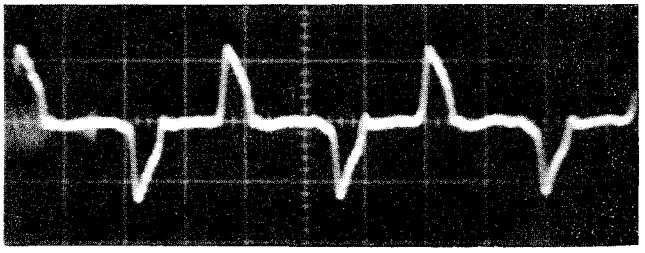

Fig. 3 Reflections of a pulse from the free ends of a steel rod, 0.313 in. diam., 36 in. long; sweep rate: 100 μsec/div.

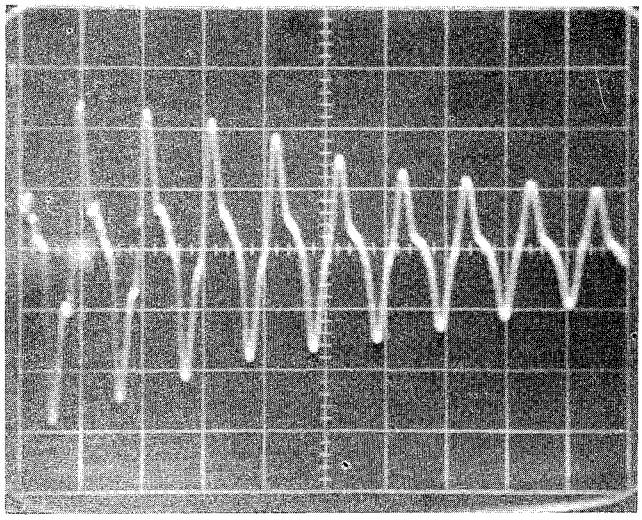

a)

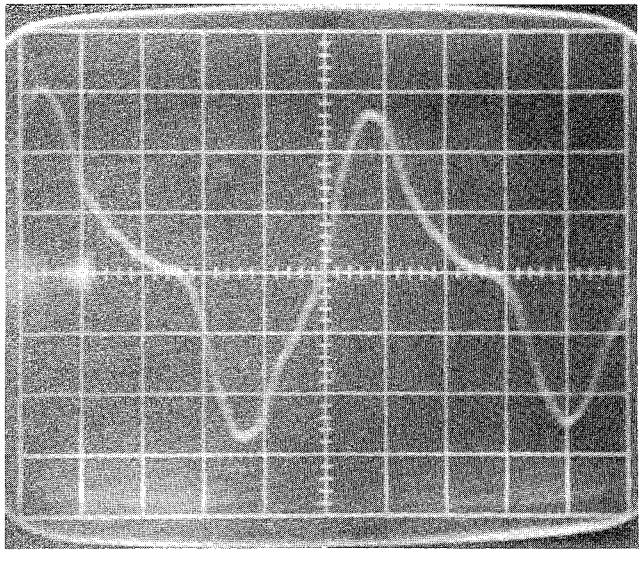

b)

Fig. 4 Reflections of a pulse from the free ends of a glass-epoxy rod, 0.315 in. diam, 10 in. long; sweep rate: a) 100 μsec/div. b) 20 μsec/div.

epoxy specimens were provided by Hamilton Standard. The latter were fabricated by hand collimmating the fibers and injection molding the resin. The mechanical properties of the boron filaments and the epoxy resin, as well as the fiber content of the resulting composite are believed to be very similar to those of the Scotchply SP-272 specimens which were used in the vibration tests.

For the purpose of comparison, the propagation of a pulse in a steel specimen was examined. A typical oscilloscope record which shows successive reflections from the free ends of the steel rod is shown in Fig. 3. The interval between two consecutive positive (compressive) or negative (tensile) peaks represents the time required for the pulse to travel a distance of twice the length of the rod; the velocity of the pulse can be determined from this transit time. Since the pulse is tensile as it travels one-half the distance and compressive during the other half, it is essentially the "flexural modulus" rather than the tensile modulus which is measured (i.e., the same modulus as that measured in the vibration tests).

Figure 4 shows oscilloscope records of the dynamic strains in a glass-epoxy rod, photographed at two different sweep rates. In this test the length of the pulse was approximately equal to the length of the specimen, and therefore the tail of one pulse slightly overlapped the beginning of the following (reflected) pulse. Attenuation of the waveform is seen to be significant. Furthermore, it is observed that any discontinuities in the waveform become less and less sharp as the pulse travels along the rod; this behavior is characteristic of viscoelastic materials.

Figure 5 shows dynamic strain records for a boron-epoxy composite. The pulse is seen to suffer much less attenuation in this specimen than in the glass-epoxy rod, but the response characteristics are otherwise similar.

We now wish to compare the velocity and attenuation of pulses in the composite rods with values predicted from the vibration data. With this in mind, let the strain ϵ at some point $x = 0$ in the rod be represented by the Fourier integral

$$\epsilon(0, t) = \int_0^\infty a(p) \cos(pt + \beta)dp \tag{3}$$

where the Fourier coefficient $a(p)$ and β define the shape of the pulse, and p denotes the circular frequency. Assuming linear viscoelastic response, the strain at a distance x from the origin is given by[11]

$$\epsilon(x, t) = \int_0^\infty a(p)e^{-\alpha x}\cos[p\,(t - x/c) + \beta]dp \tag{4}$$

Table 3 Vibration data for boron-epoxy specimens

Specimen	10 ply, 0°				10 ply, 90°				9 ply, 0°-90° (crossply)			
Mode	f_n, cps	f_n/f_1	$E_1 \times 10^{-6}$, psi	$\tan\delta \times 10^2$	f_n, cps	f_n/f_1	$E_1 \times 10^{-6}$, psi	$\tan\delta \times 10^2$	f_n, cps	f_n/f_1	$E_1 \times 10^{-6}$, psi	$\tan\delta \times 10^2$
1	48.2	1.0	27.9	—	16.2	1.0	3.10	—	37.2	1.0	18.4	—
2	298	6.20	27.2	—	101	6.24	3.07	—	231	6.22	18.0	—
3	829	17.2	26.8	0.32	283	17.5	3.07	2.3	642	17.3	17.8	0.35
4	1650	34.3	27.6	0.48	563	34.8	3.18	2.4	1290	34.7	18.6	0.35
5	2690	55.8	27.0	0.51	931	57.4	3.18	2.4	2110	56.8	18.4	0.38
6	4000	83.0	26.8	0.67	1400	86.5	3.23	2.8	3100	83.4	17.9	0.48
7	5620	117	27.1	0.64	1960	121	3.26	3.2	4390	118	18.3	0.57
8	7400	154	26.7	0.80	2600	160	3.23	3.2	5810	156	18.1	0.64
9	9400	196	26.2	1.00	3300	204	3.15	3.2	7310	197	17.5	0.89
10					4710	257	3.24	3.3	9180	247	17.6	0.89
11					5090	314	3.25	3.6				
12					6130	379	3.29	3.9				
13					7220	446	3.23	4.3				
14					8430	521	3.29	—				
15					9620	594	3.23	—				

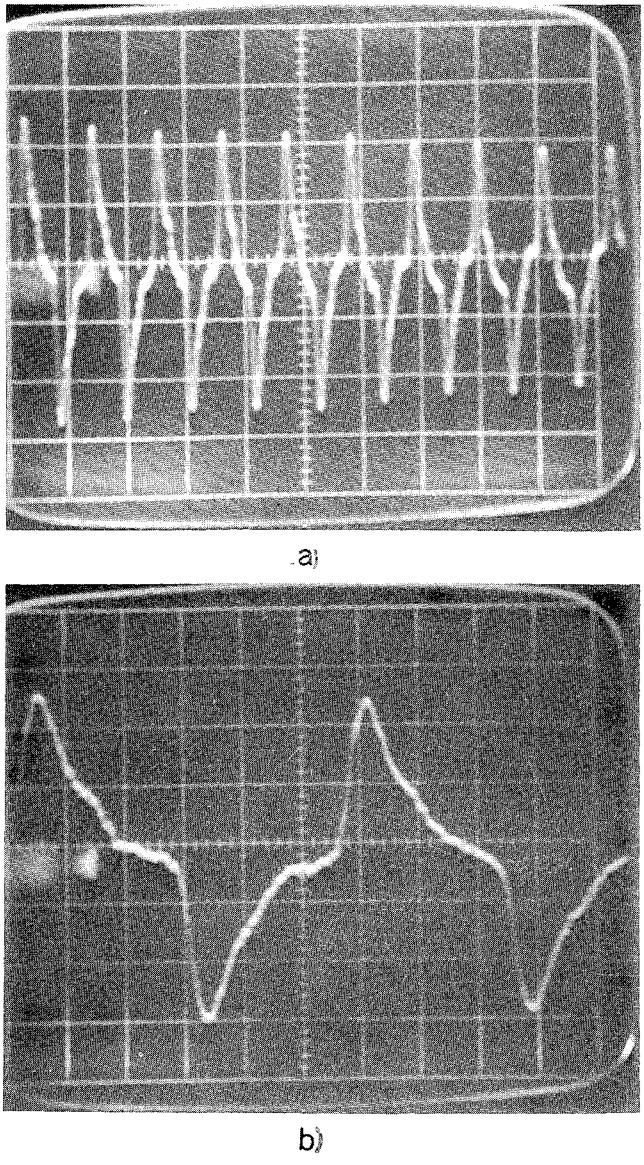

Fig. 5 Reflections of a pulse from the free ends of a boron-epoxy rod, 0.210 in. diam, 24 in. long; sweep rate: a) 100 μsec/div. b) 20 μsec/div.

where the phase velocity c and the attenuation coefficient α are

$$c = (|E^*|/\rho)^{1/2} \sec(\delta/2)$$
$$\alpha = (p/c) \tan(\delta/2) \tag{5}$$

For materials having a small loss factor ($\tan\delta \ll 1$), c and α have the approximate values

$$c \approx (E_1/\rho)^{1/2}, \quad \alpha \approx (p/2c) \tan\delta \tag{6}$$

Hence, by knowing E_1 and $\tan\delta$ for the composite materials, one can compute c and α using Eq. (6), and then evaluate the strain ϵ by numerically integrating the integral in Eq. (4).

Table 4 Modulus, $E_1 \times 10^{-6}$, psi

Method	Glass-epoxy	Boron-epoxy
Resonance (fundmental mode)	5.17	27.9
Pulse-propagation (impact)	5.18	30.2
Static measured	5.10	29.5
Rule-of-mixtures	5.00	30.5

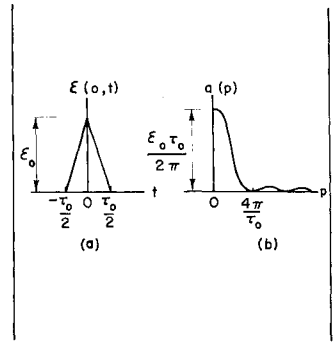

Fig. 6 a) Assumed shape of pulse, b) Fourier coefficient of the pulse.

We recall that E_1 (and therefore c) varies only slightly with frequency for the composite materials investigated, although $\tan\delta$ (and α) is strongly frequency dependent. The values of E_1 measured in the vibration tests and those computed from the velocity of propagation using Eq. (6) are compared in Table 4. The agreement is seen to be relatively good, considering the fact that different specimens were used in each of the two tests.

Also reported in Table 4 are the static moduli of the composite rods, and values of E_1 based upon the classical "rule-of-mixtures." The static modulus was determined by hanging known weights on cantilever beam specimens and recording the strain with etched-foil gages. These static values are seen to be slightly smaller than the corresponding dynamic ones. The rule-of-mixtures modulus represents the value of E_1 computed from data published by the manufacturer, according to $E_1 = v_f E_f + v_m E_m$ where v is the volume fraction and subscripts f and m denote the filament and matrix materials, respectively. Since the properties of the constituent materials are not known precisely, these values are shown merely as a matter of interest.

In order to predict the attenuation of a pulse its shape must be specified. For convenience the pulse is assumed to have the triangular form shown in Fig. 6a. Then $\beta = 0$ and the Fourier coefficient $a(p)$ (Fig. 6b) is given by

$$a(p) = (4\epsilon_0/\pi p^2 \tau_0)[1 - \cos(p\tau_0/2)] \tag{7}$$

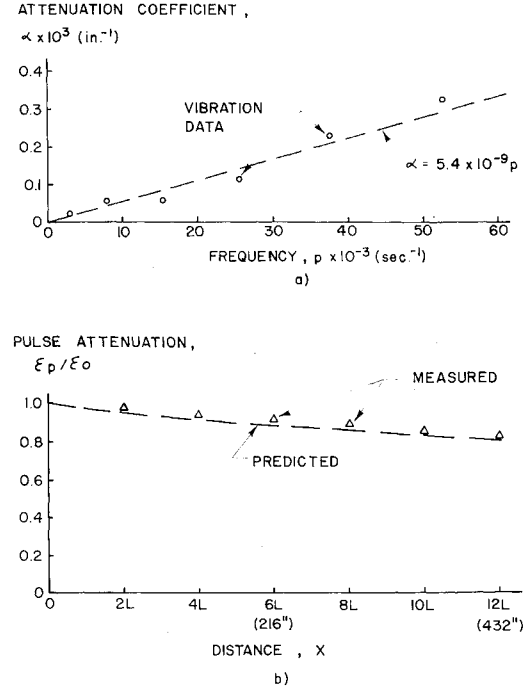

Fig. 7 Attenuation in a steel specimen.

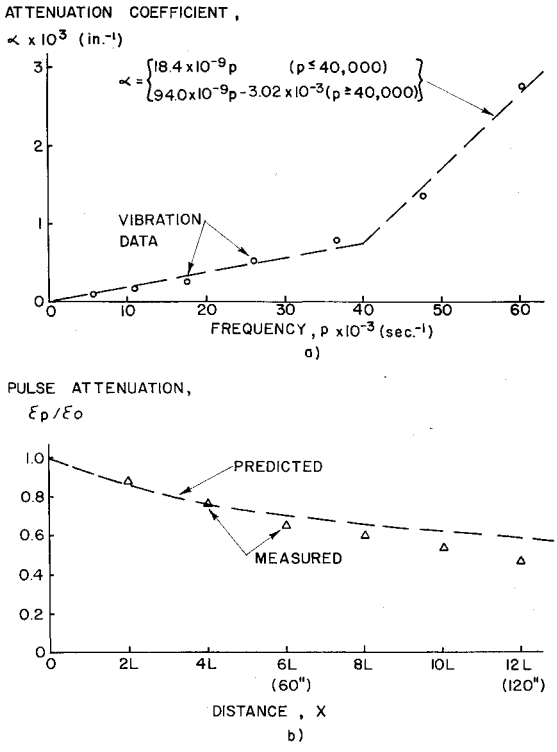

Fig. 8 Attenuation in a glass-epoxy specimen.

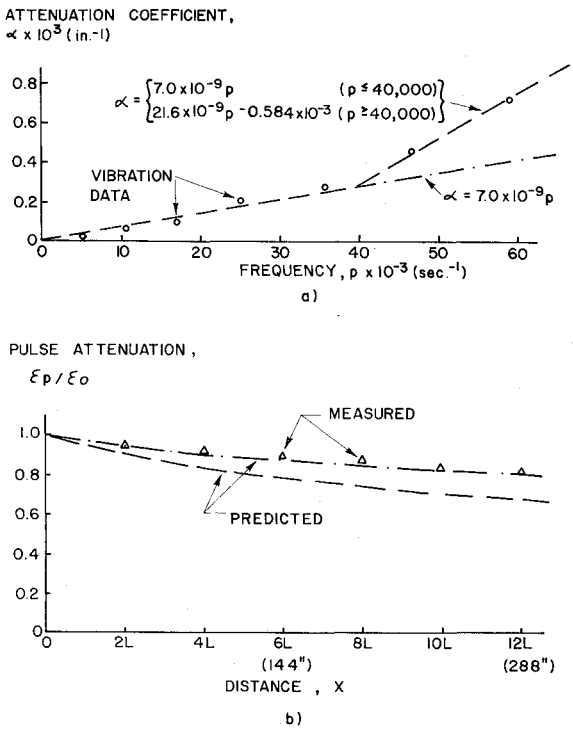

Fig. 9 Attenuation in a boron-epoxy specimen.

Substituting Eq. (7) into Eq. (4) gives

$$\epsilon(x,t) = \int_0^\infty \frac{4\epsilon_0[1 - \cos(p\tau_0/2)]}{\pi p^2 \tau_0} e^{-\alpha x} \cos\left[p\left(t - \frac{x}{c}\right)\right] dp \tag{8}$$

The maximum value of the strain $\epsilon_p(x)$ at a distance x along the rod occurs when the cosine term in Eq. (8) is equal to unity, in which case

$$\frac{\epsilon_p(x)}{\epsilon_0} = \int_0^\infty \frac{4[1 - \cos(p\tau_0/2)]}{\pi p^2 \tau_0} e^{-\alpha x} dp \tag{9}$$

This expression can be integrated numerically in order to find the pulse attenuation ratio $\epsilon_p(x)/\epsilon_0$. It should be noted that Eq. (9) requires that the attenuation coefficient α be specified over an infinite frequency range, whereas the vibration tests supply data up to only 10,000 cps. It was found, for example, that for zero attenuation and a pulse duration of $\tau_0 = 50\mu$sec, that the frequency range (0–10,000 cps) provides only 50% of the dynamic response. Hence it was necessary to extrapolate the known data; a linear extrapolation of α was used in all cases investigated below. Furthermore the region of integration was taken as $0 \le p \le 10^7$ sec^{-1}. It was verified that frequency components larger that 10^7 sec^{-1} contributed less than 0.3% to the dynamic response.

The attenuation coefficient for steel, computed from the vibration data (Table 1) using Eq. (6), are shown as circles in Fig. 7a. Rather than curve fitting these points exactly, the dotted line shown was chosen to represent the function α.§

§ The assumption that α is proportional to the frequency p is equivalent to the assumption that tanδ is a constant (since c is approximately constant). From Table 1 it is clear that tanδ is somewhat frequency dependent. Such an assumption is consistent, however, with Kolsky's observations Eq. (12) that for many real viscoelastic material tanδ varies little with frequency. This implies that constitutive equations based upon simple viscoelastic models (e.g., Maxwell or Kelvin) are of little use in predicting damping of these materials, since such models predict large variations of tanδ with frequency.

The resulting pulse attenuation ratio ϵ_p/ϵ_0, drawn as a dotted line in Fig. 7b, agrees extremely well with the measured values for the range of x considered.

Vibration data for the glass-epoxy composite are plotted in Fig. 8a. In this case a bilinear function was chosen to represent the coefficient α. Although the resulting pulse attenuation ratio is in good agreement with the measured values at short distances, it predicts too little attenuation for large x.

Figure 9 shows similar curves for the boron-epoxy material. In this case, however, the bilinear function chosen to represent the vibration data predicted greater pulse attenuation than that which was measured experimentally. Quite possibly the damping associated with the higher frequencies ($p >$ 60,000 sec^{-1}) was actually less than the extrapolated values of damping used in the numerical integration. For example, if the straight line $\alpha = 7.0 \times 10^{-9}p$ (shown as a dash-dot line) is used, the agreement is seen to be greatly improved. Furthermore, in making this comparison, it must be remembered that different boron-epoxy specimens were used in the two tests.

IV. Ultrasonic Tests

A limited number of ultrasonic tests have been performed as part of a long-range investigation on the use of ultrasonics for studying the dynamic behavior of composite materials. The apparatus which was used in this pilot study is shown in Fig. 10. An Arenberg oscillator (model PG-650) was used to generate an ultrasonic pulse, which was introduced into the composite by means of a piezoelectric ceramic transducer (lead zirconate-titanate). An identical crystal bonded to the

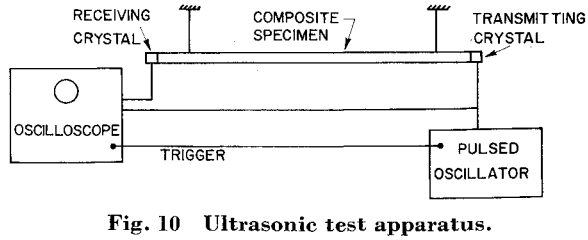

Fig. 10 Ultrasonic test apparatus.

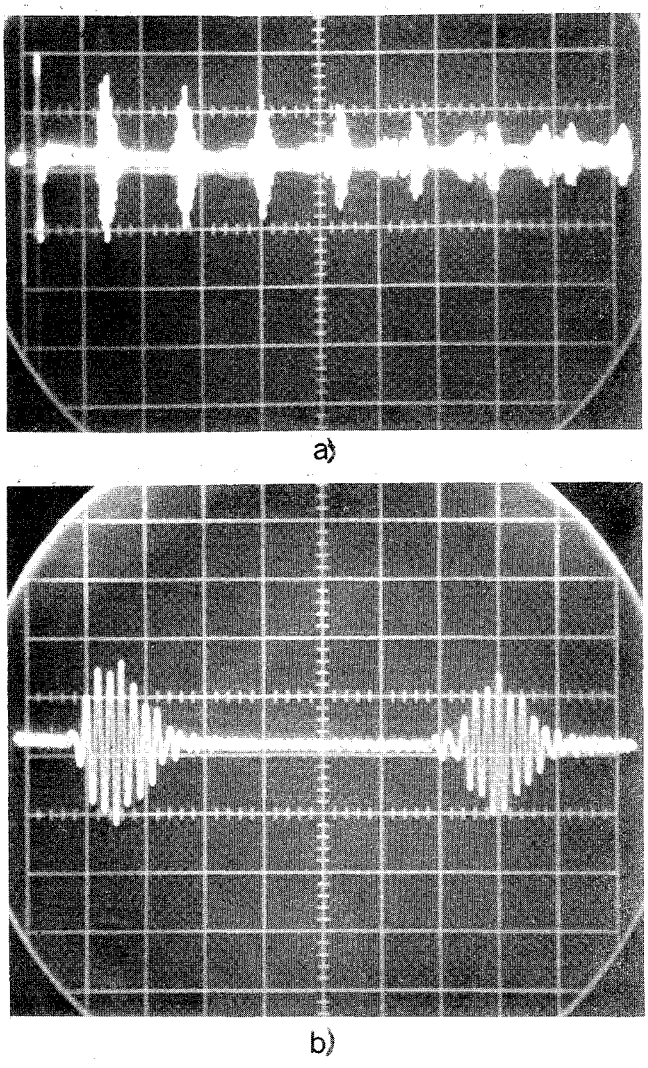

Fig. 11 Echoes of an ultrasonic pulse in a steel rod, frequency, f = 0.25 mHz; sweep rates: a) 100 μsec/div. b) 20 μsec/div.

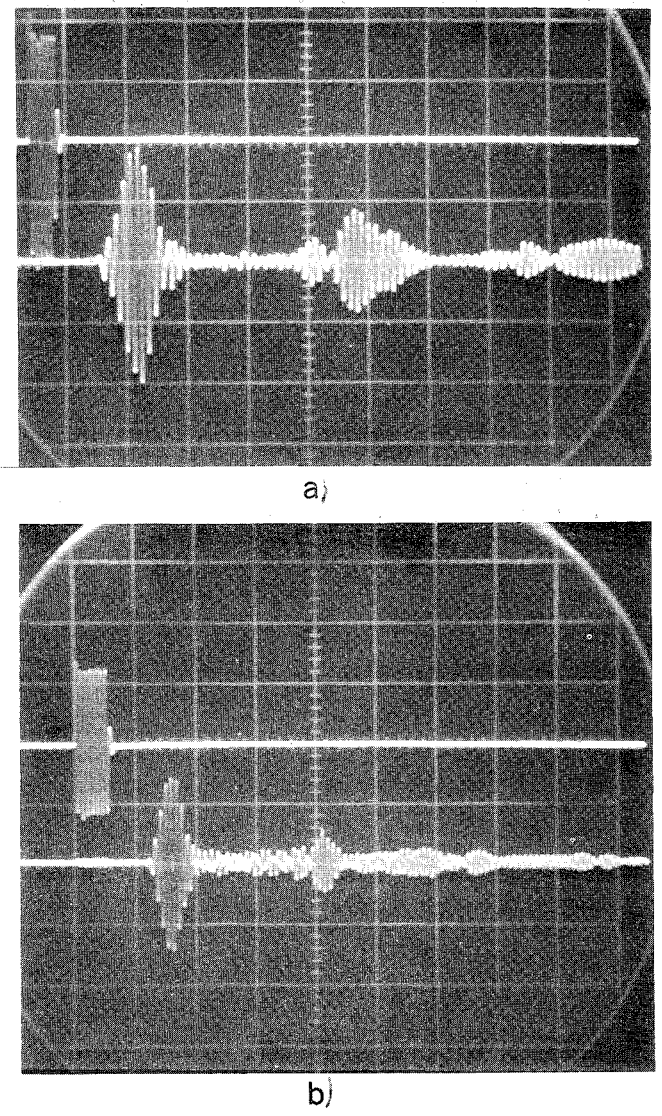

Fig. 12 Ultrasonic pulses in composite rods, frequency f = 0.25 mHz. Sweep rate: 50μ sec/div; a) glass-epoxy rod, 0.315 in. diam, 10.0 in. long; b) boron-epoxy rod, 0.210 in. diam, 22.85 in. long.

opposite end of the specimen was used as the receiving transducer, or, in some cases, the same crystal was employed both to transmit and receive the pulse.

Typical oscilloscope records which show reflections (or echoes) of an ultrasonic pulse from the ends of a steel rod are given in Fig. 11. The time scale has been expanded in the second photograph in order to show the detail of the first and second reflections. A single transducer was used to transmit the pulse and to record the reflections. Hence the interval between consecutive peaks represents the time required for the pulse to travel twice the length of the rod.

Figure 12 shows similar records for glass-epoxy and boron-epoxy rods. In these tests separate transducers were used, one to generate the pulse (top trace) and the other to receive the transmitted pulse (lower trace). It is seen that although the first received pulse is well defined, subsequent echoes are much less distinct. The additional reflections which are observed may be the result of slightly rough or nonparallel surfaces at the ends of the specimen. They may also be due to the presence of the crystals themselves; i.e., a significant portion of the energy may be transmitted through the interface and into the crystal when the pulse reaches the end of the rod. It is possible, however, to determine the speed of propagation by measuring the time interval between the initiation of the original pulse (top trace) and its arrival at the opposite end of the bar (lower trace). These speeds are recorded in Table 5, where it is seen that the high-frequency pulses (0.25 mHz) have approximately the same velocity as the lower-frequency pulses generated in the impact tests. This indicates that dispersion (the dependence of velocity upon frequency) is rather insignificant even at frequencies of 0.25 mHz. It might be mentioned that, on the basis of the Pochhammer-Chree solution for elastic bars,[13] geometric dispersion is negligible when the ratio of the bar's radius to the relevant wavelength ($\lambda = c/f$) is less than 0.1. This ratio is approximately 0.1 for both the steel and boron-epoxy specimens, but somewhat higher (0.2) for the glass-epoxy rod. No dispersion (geometric or material) is apparent in the frequency range considered so far; however further research in this area is presently being carried out.

Table 5 Velocity of propagation, $c \times 10^{-6}$, in./sec

Method	Steel	Glass-epoxy	Boron-epoxy
Impact	0.202	0.176	0.412
Ultrasonic (0.25 mhz.)	0.201	0.179	0.398

V. Conclusions

It has been demonstrated that distinct stress pulses can be generated and observed in fiber-reinforced epoxy rods. By

knowing the effective elastic and damping properties of the materials over a sufficiently large frequency range the speed and attenuation of the pulses can be predicted using the linear theory of viscoelasticity.

Material dispersion appears to be relatively insignificant in glass-epoxy and boron-epoxy samples below 0.25 mHz, although further research in this area is needed. Ultrasonic methods have been shown to provide a useful way of studying dispersion in composite materials.

In this paper attention has been restricted to disturbances propagating in the direction of the reinforcing filaments. A complete characterization of the dynamic behavior of unidirectional fiber-reinforced materials requires a knowledge of the remaining four dynamic moduli (assuming transverse isotropy). Hence additional testing is needed.

References

[1] Schultz, A. B. and Tsai, S. W., "Dynamic Moduli and Damping Ratios in Fiber-Reinforced Composites," *Journal of Composite Materials*, Vol. 2, 1968, p. 368.

[2] Schultz, A. B. and Tsai, S. W., "Measurements of Complex Dynamic Moduli for Laminated Fiber-Reinforced Composites," *Journal of Composite Materials*, Vol. 3, 1969, p. 434.

[3] Abbott, B. W. and Broutman, L. J., "Stress-Wave Propagation in Composite Materials," *Experimental Mechanics*, Vol. 6, 1966, p. 383.

[4] Lifshitz, J. M., "Specimen Preparation and Preliminary Results in a Study of the Mechanical Properties of Fiber Reinforced Materials," MML Rept. 15, Jan. 1969, Israel Inst. of Technology.

[5] Kolsky, H., "The Propagation of Stress Pulses in Viscoelastic Solids," *Philosophical Magazine*, Vol. 1, 1956, p. 693.

[6] Bodner, S. R. and Kolsky, H., "Stress Wave Propagation in Lead," *Proceedings of the 3rd U.S. National Congress of Applied Mechanics*, 1958, p. 495.

[7] Asay, J. R., Dorr, A. J., Arnold, N. D., and Guenther, A. H., "Ultrasonic Wave Velocity-Temperature Studies in Several Plastics, Plastic Foams and Nose-Cone Materials," AFWL-TR-188, March 1966, Air Force Weapons Lab.

[8] Asay, J. R., Urzendowski, J. R. and Guenther, A. H., "Ultrasonic and Thermal Studies of Selected Plastics, Laminated Materials, and Metals," AFWL-TR-67-91, Jan. 1968, Air Force Weapons Lab.

[9] Timoshenko, S., Vibration Problems in Engineering, 3rd ed., D. Van Nostrand, New York, 1955, p. 334.

[10] Pao, Y. H. and Kowal, C., "A Laboratory for Teaching Mechanical Vibrations," *Journal of Engineering Education*, Vol. 56, 1965, p. 96.

[11] Kolsky, H., "Viscoelastic Waves," *International Symposium on Stress Wave Propagation in Materials*, edited by N. Davids, Interscience, New York, 1960, p. 59.

[12] Kolsky, H., "The Propagation of Mechanical Pulses in Anelastic Solids," *Behavior of Materials under Dynamic Loading*, edited by N. J. Huffington, Jr., ASME, 1965.

[13] Kolsky, N., *Stress Waves in Solids*, Dover, New York, 1963, p. 54.

AUGUST 1971 AIAA JOURNAL VOL. 9, NO. 8

Crossflow and Unsteady Boundary-Layer Effects on Rotating Blades

H. A. DWYER*
University of California, Davis, Calif.

AND

W. J. MCCROSKEY†
U. S. Army Aeronautical Research Laboratory, Moffett Field, Calif.

Laminar viscous flow on propellers and helicopter rotors has been studied for a wide variety of blade shapes and environments. The significance of crossflow and unsteady effects has been assessed, and the physical processes which influence the primary flow around the blade have been explained. Special attention has been devoted to those terms in the differential equations that change the boundary-layer structure from that of two-dimensional steady flow. Detailed analyses and calculations reveal that large rotational effects are limited to the immediate vicinity of the rotor hub, while the unsteady and yawed-wing effects of forward flight are important over most of the blade surface. However, chordwise pressure gradients tend to predominate over rotational and unsteady velocity effects for blunt bodies or thin airfoils at large angles of attack. Experimental results for laminar separation and transition support these predictions.

I. Introduction

SOME of the least understood and most important problems in fluid flow are associated with the three-dimensional and time-dependent environments that exist in the real world. The reasons for this lack of understanding are basically twofold: 1) there is a general lack of analytical and numerical techniques available which can handle three-dimensional and time-dependent problems; and 2) experimental measurement techniques are primarily two-dimensional and steady. In this paper the important practical problem of boundary-layer flow over a helicopter rotor is tackled analytically and experimentally. The rotor problem has many three-dimensional features in common with geophysical flows, turbine blades, propellers and rotating machinery, and it also contains a strong time-dependent characteristic. Therefore, a fundamental attack on the helicopter rotor problem is of general interest to many areas of fluid dynamics.

The problems involved with helicopter rotors can best be explained with the help of Fig. 1. The most general rotor

Presented as Paper 70-50 at the AIAA 8th Aerospace Sciences Meeting, New York, Jan. 19–21, 1971; submitted February 20, 1970; revision received January 25, 1971.

Index Categories: Rotary Wing and VTOL Aerodynamics; Boundary Layers and Convective Heat Transfer—Laminar; Nonsteady Aerodynamics.

* Associate Professor, Member AIAA.

† Research Scientist, Member AIAA.